

Evolution of Double Vortices Induce Tropical Cyclogenesis of Seroja over Flores, Indonesia

Erma Yulihastin (✉ erma005@brin.go.id)

Indonesian National Institute of Aeronautics and Space: Lembaga Penerbangan dan Antariksa Nasional
<https://orcid.org/0000-0001-5327-7597>

Ankiq Taofiqorahman

Universitas Padjadjaran Kampus Jatinangor: Universitas Padjadjaran

Ibnu Fathrio

Lembaga Penerbangan dan Antariksa Nasional

Fadli Nauval

Lembaga Penerbangan dan Antariksa Nasional

Dita Fatria Andarini

Lembaga Penerbangan dan Antariksa Nasional

Rahaden Bagas Hatmaja

Lembaga Penerbangan dan Antariksa Nasional

Akhmad Fahim

Badan Meteorologi dan Geofisika: Badan Meteorologi Klimatologi dan Geofisika

Namira Nasywa Perdani

Universitas Padjadjaran Kampus Jatinangor: Universitas Padjadjaran

Haries Satyawardhana

Lembaga Penerbangan dan Antariksa Nasional

M. Furqon Azis Ismail

Lembaga Ilmu Pengetahuan Indonesia

Dwiyoga Nugroho

Republik Indonesia Kementerian Kelautan dan Perikanan

Suaydhi -

Lembaga Penerbangan dan Antariksa Nasional

Iis Sofiati

Lembaga Penerbangan dan Antariksa Nasional

Lely Qodrita

Lembaga Penerbangan dan Antariksa Nasional

Herlina Ika Rahmawati

Republik Indonesia Kementerian Kelautan dan Perikanan

Research Article

Keywords: tropical cyclogenesis, Indonesia Maritime Continent, MJO, equatorial Rossby, double vortices

Posted Date: July 12th, 2022

DOI: <https://doi.org/10.21203/rs.3.rs-1774818/v1>

License:  This work is licensed under a Creative Commons Attribution 4.0 International License.

[Read Full License](#)

Abstract

Over one hundred years of vigorous progress in tropical cyclone (TC) research, the genesis of the cyclone (hereafter, tropical cyclogenesis) is remarkable as a doubtful subject. Furthermore, predicting tropical cyclogenesis, particularly in the lesser latitude, remains a significant challenge. Therefore, understanding the complex interactions in developing tropical cyclogenesis over the region is vital to improving tropical cyclogenesis forecasting. Hence, the Indonesia Maritime Continent is a tropical cyclone-free region due to decreasing the Coriolis effect. However, Seroja TC hits Flores (8.6° S, 120° E), east Nusa Tenggara, Indonesia, on 4 April 2021, and recorded as the first TC occurred over the mainland, which brought a catastrophic disaster in the region. This study investigated the tropical cyclogenesis of Seroja by using both observational and numerical studies. The results indicate that a marine heatwave and double vortices were favorable conditions produced preconditions to developing tropical cyclogenesis over the Maluku Sea. Thus, tropical cyclogenesis is formed by the breakdown of the intertropical convergence zone (ITCZ) associated with synoptic-scale wave train driven under the interaction of the Madden Julian oscillation (MJO) and equatorial Rossby waves. Moreover, our finding suggested that an extensive background cyclonic vorticity under the cold pool mechanisms is responsible for maintaining tropical cyclogenesis into a persistent Seroja TC.

1 Introduction

Genesis of the tropical cyclone (hereafter, tropical cyclogenesis) was defined as the possibility of the tropical storm will endure evolving from this point favor and further turn into self-sustaining. Thus, tropical cyclogenesis comprises dynamic and thermodynamic processes and its interaction at multiple spatio-temporal scales [1]. In term of external processes, tropical cyclogenesis may be induced by large scale circulations [2] (i.e., monsoon [3]), intertropical convergence zone [5]; [6], Madden Julian Oscillation (MJO) [7]; [8]; [9], equatorial waves [7]; [9], and proven by recently previous work that the activity (i.e., MJO) determined by the dynamic of regional ocean [10] and depend on moisture advection over Indo-western Pacific [11]. As a result, predicting genesis of TC prevails uncertain [12] despite significant progress in understanding interaction between tropical cyclones (TC) and their environment which affect to its intensity and structure [1].

Tropical cyclogenesis over the Indonesia Maritime Continent (8° N– 10° S; 90° – 150° E) was less documented due to the diminishing Coriolis effect in the region. However, Typhoon Vamei existed over near Singapore (1.5° N) on 27 December 2001, which was caused of the interaction between weak Borneo Vortex and strong-persistently northerly surge [13]. Moreover, these long-lasting northerly surges, which frequently occur from October to March, have proven statistically associated with the tropical cyclones over the eastern Indian Ocean-Maritime Continent sector [14]. Nevertheless, it is important to notice that contribution of the Asian monsoon activity is less during March-to-April so that no tropical cyclones associated with northerly surges were reported occurred over the region [14].

However, the Seroja tropical cyclone occurred on 4 April 2021 over Flores, east Nusa Tenggara, Indonesia, and was recorded by the Tropical Cyclone Warning Center (TCWC) as the first tropical cyclone over the mainland in the Maritime Continent region (see: Fig. 1). The 3-level cyclone killed 181 people, injured 47 people, evacuated 9,449 people, missed 72 people, and destroyed 1.962 infrastructures [15]. During that period, the western Maritime Continent had less tropical disturbance related to vorticity activity over the Borneo region which is identified as the most triggered the tropical vortices [16] in the Maritime Continent (see: Fig. 2). On the other hand, double vortices were exhibited over the eastern Maritime Continent, particularly over the Maluku Sea to the north and the Banda Sea to the south from 27 March to 31 March 2021 (Fig. 2).

Regarding the hypothesis that double vortices over the eastern seas of the Maritime Continent may contribute to developing tropical cyclogenesis, we conducted observation and numerical studies to investigate the physical and dynamic processes. Due to limited observation over eastern Indonesia, we combined observation from both satellite and reanalysis data. Moreover, we use a high-resolution numerical weather prediction model of the Weather Research and Forecasting (WRF) model at a 3 km spatial resolution to explore how dynamical processes control the tropical cyclogenesis over the low-level atmosphere over central and eastern Indonesia (104.25° E– 136.57° E, 11° S– 10.4° N)

2 Materials And Methods

The methods applied in this study combine observational and numerical approaches to investigate the tropical cyclogenesis process. First, we perform statistical analysis using spatial, time series, and Hovmöller diagrams from both satellites and high-resolution reanalysis data to confirm the anomalies signals of physical processes in the meso-to-large scales. Furtherly, we conduct numerical studies to explore the dynamic process that may control the tropical cyclogenesis in the local-to-regional regions of eastern Indonesia.

The statistical-based analysis was performed using the Himawari [17] and the Global Satellite Mapping of Precipitation (GSMaP) [18], the cross-calibrated multiple (CCMP) [19]; [20]), and the European Centre for Medium-Range Weather Forecasts (ECMWF) reanalysis of ERA5 datasets [21] with have spatial resolutions of 0.05° , 0.1° , 0.05° , and 0.05° , respectively. To identify tropical cyclogenesis, we explored convective activity, convergence region, low-pressure system, and potential vorticity through data parameters of Blackbody Temperature (TBB) of cloud, outgoing longwave radiation (OLR), precipitation, sea surface temperature, surface wind, and water vapor. Furthermore, to explore preconditioning of the tropical cyclogenesis over the internal sea of eastern Indonesia (i.e., Maluku Sea), we examine a short marine heatwave (MHW) phenomenon using criteria of 90th percentile during 40-day time window following [22].

We then performed a numerical simulation using the Weather Research and Forecasting (WRF) model version 4.2.1 [23] with initial and boundary conditions derived from ERA5 with a spatial and temporal resolution 0.25° and 6 h. The WRF model configuration (Table 1) following [24], who succeeded in

simulating precipitation in intensity, and has proven that the configuration could capture heavy rainfall events in maximum intensity, timing, duration, and location [25 [26] with around two hours phase early. In this numerical study, we simulated selected episodes of tropical cyclone events from 31 March to 6 April 2021 with a lead time of 12 hours is considered an appropriate spin-up time for the model.

Table 1

Model configuration (following Fonseca et al. 2015) [24] used in this study for the simulation of tropical cyclogenesis over eastern Maritime Continent (see Fig. 1 for the spatial domain configuration) with input and boundary conditions derived from ERA5 data of 0.25° spatial resolution.

Parameterization	Betts–Miller– Janji’c (BMJ) Scheme
	D01 (3km)
Number of horizontal grids	1200 x 800
Number of vertical grids	33
Cumulus	BMJ
Microphysics	WDM5
PBL	WSM-3
SW-Radiation	RRTM/Dhudia
LW-Radiation	RRTM/Dhudia
Boundary Layer	Yonsei University
Surface Layer	Revised MM5 Monin-Obukhov
Land Surface	NOAH

3 Result And Discussion

3.1 Precondition of Seroja Tropical Cyclogenesis

Precondition of Seroja tropical cyclogenesis started from ten days (day–10) before the cyclone initiated on 4 April 2021 (hereafter denoted as day–0, see: Fig. 1). Development of tropical depression over the eastern sea of Indonesia (20° S–10° N, 120–140° E) was captured by the existence of anti-cyclonic vortex (convergence) over the northern part (Eq–10° N) and cyclonic vortex (divergence) over southern part (20° S–10° S) near Australia (Fig. 2a). This feature explained by previous work as Equatorial Rossby (ER), which associated with positive moisture flux convergence and westward propagation [27]. On the other hand, a pair of convergence exhibited over the Indian Ocean may be related to the 3-D structure of MJO dynamic over low-level atmosphere [28]; [29] (see: Fig. 2a).

Those double vortices over Indian Ocean develop progressively and multiply by two become four vortices on day-8. In addition, the vortex over the Maluku Sea in the north also became strong and triggered a new vortex over Banda Sea in the south (Fig. 2b). Thus, this double vortices over eastern Indonesia may sustain developing into a tropical storm in the south that is expected to be the tropical cyclogenesis of Seroja. Interestingly, on day-6, four vortices over the Indian Ocean tend to dissipate, but as a result, it produces strong eastward propagation elongated equator region (60–120° E) (Fig. 2c).

At the same time, westward propagation induced by ER activity occurred over the southeast part of Indonesia (20–10° S, 120–140° E). As the interaction between MJO and ER manifested westward and eastward collocated over central Indonesia (100–120° E), thus, it created a tropical storm in the region which intensified develop into a tropical cyclone on day-4 (Fig. 2d). On the other hand, the southern vortex over the Banda Sea also creates a tropical storm that sustains evolution as a tropical cyclone on day-0 (Fig. 2d-f). To clarify the development process of double vortices over the Maluku-Banda Sea, we then plotted the growth of the tropical cyclogenesis over eastern Indonesia in Fig. 3.

The double vortices, hereinafter north-vortex (Eq–5° N, Pacific Ocean) and south-vortex (5° S–Eq, Maluku-Banda Seas), located close to equator initiated from day-10 (Fig. 3a) over eastern Indonesia. The south-vortex remains stronger as well as larger on day-8 (Fig. 3b) and followed by creating meso-convergence over entire eastern Indonesia on day-6 (Fig. 3c). The south-vortex over the Banda Sea developed aggressively to be a tropical storm and shifted to the south close to the eastern Nusa Tenggara region (5–15° S, 120–128° E) on day-4 (Fig. 3d). Development from a tropical storm to be a tropical cyclone occurred from day-4 to day-0 (Fig. 3d-f) triggered strong wind and flash flood with the devastating impact over Flores, east Nusa Tenggara, Indonesia.

The long-lasting south-vortex over the Banda Sea (> 10 days) raised an issue regarding possible factors contributing to developing and maintaining the vortex. Therefore, we further identified sea surface temperature (SST) over the Banda Sea. We found that warming SST occurred from 15 March 2021, and a significant increase was associated with a short marine heatwave (MHW) initiated from 21–27 March 2021 (Fig. 4). It is important to notice that MHW is notable as a progressive issue under global warming which detected an increase in term intensity, duration, and frequency [30].

The MHW also recorded as factor drives extreme rainfall triggered severe flooding during Australia summer of 2018–2019 [31]. In this event, MHW during 21–27 March may provide a favorable environment for preconditioning of tropical cyclogenesis with the development of double vortices over Maluku Sea in the north and the Banda Sea in the south that turn into the mature stage on 29–30 March 2021 (Fig. 5). Hence, we need to clarify the relationship between north-vortex and south-vortex and how the north-vortex contribute to maintain the long-lasting south-vortex.

3.2 MJO-ER Interaction Induced Tropical Cyclogenesis

From 29 March 2021 in the morning, the strong southerly wind occurred over low-level troposphere (< 700 mb), and the cyclonic vorticity developed in the upper-level troposphere (> 500 mb). Conversely, on the

north side, the high positive anomaly of potential vorticity (PV) occurred in the top level of the troposphere (> 100 mb). Hence, the stratospheric air penetrated the troposphere creating a strong anti-cyclonic vortex. This large north-vortex has a significant growth with strong updraft from the surface to the top-troposphere, which developed over the equatorial region, thus, created two small vorticities over the middle troposphere in the south (10° S–Eq).

Those small vortices produce the large and adequate south-vortex, clearly displayed on 29 March at 18:00 LST (Figure not shown). The strong connection between the north-to-south vortices remains enduring until 30 March 2021 at 11:00 LST. In this case, with a rough calculation, the maximum of meridional surface wind for the north-vortex and the south-vortex are 8 m s^{-1} and 6 m s^{-1} , respectively. Thus, these values are above the wind speed threshold, which is needed for the initial vortex to endure the convection during the genesis period, as mentioned in the previous study [32].

These interactions between two vortices are notable as a second factor influencing Seroja tropical cyclogenesis's preconditioning. In addition, the south-vortex is also supported by the existence of a double intertropical convergence zone (ITCZ) which provides a large convergence zone over the southern region near the equator (10° S–Eq), despite on April the ITCZ suggested existed over northern Hemisphere. It is consistent with previous studies that have mentioned the relationship between double ITCZ phenomena [33]; [34] and tropical cyclogenesis [6]. In this case, the tropical cyclogenesis is formed by the breakdown of the south ITCZ associated with synoptic-scale wave train driven under the interaction of the Madden Julian oscillation (MJO) and equatorial Rossby waves.

Furtherly, to confirm the time evolution of the double vortices over the surface level, we explored several parameters and used the Hovmöller diagrams to analyze the features in longitudinal and latitudinal orientations (Fig. 6). Figure 6a shows that the north of mesoscale convergence associated with the north-vortex occurred early on 19 March 2021, followed by the south-vortex on 25 March 2021, which corresponds to the ER activity signed by collocated of convergent regions [27]. This event is supported by the high positive anomaly of PV that occurred over the northern regions (Eq– 15° N) from 19 March 2021 (Fig. 6b). This ER existence is also described by the westward propagation of convective activity and total water vapor column from around 22 March 2021 (Fig. 6c-d). On the other hand, the MJO phase 4 produced a strong eastward propagation of convective regions and may interact with ER over around 110 – 120° E (see: Fig. 6c-d, the black dashed-boxes). However, a numerical study is needed to investigate how the dynamics aspect controls the interaction by intensifying convective activity and accumulation precipitation over the limited area (110 – 120° E) that will be presented in the further figures.

3.3 Dynamic Controls of Seroja Tropical Cyclogenesis

To study the dynamic controls of tropical cyclogenesis over surface-level using the WRF model, we need to compare the precipitation simulated by the model with the precipitation observed by the GSMaP satellite data (Fig. 7) during 3–4 April 2021. Because our primary focus is to understand the dynamic

process over the area interest due to location attributed to the interaction between MJO and ER, we analyze rainfall evolution over the limited area of $10\text{--}3.5^\circ\text{ S}$, $110\text{--}120^\circ\text{ E}$ (red box, Fig. 7).

On the other hand, the relationship between the north and south vortices over the surface ($< 1\text{ km}$) may also control the tropical cyclogenesis by enhancing the upward motion over the equatorial region (Fig. 12). The intensification of upward motion has a strong connection with the north (D , 10° N) induced by a cold pool (CP), which is identified by a low potential temperature (blue contour line) over surface-level ($< 1\text{ km}$). The CP as part of a mesoscale vortex tends to be a quasi-stationary system that also supports maintaining the tropical cyclogenesis over the south (C , 10° S). On 4 April 2021, the CP (hereafter, north-CP) extend to the south and propagates, also produce a new CP over equator (hereafter equator-CP).

The evolution of the dynamic process of the CPs during the tropical cyclone event is depicted in Fig. 13, which is easily described as follows. The north-CP starts developing from early morning at 01:00 LST on 4 April 2021 (Fig. 13a). The extension of the north-CP induced a new convection cell in the south (5° N), and the equator-CP developed at 02:00 LST on 4 April 2021. Furtherly, the north-CP created several convections which intensify elongated from the Equator to the north (D , 10° N) at 04:00 LST on 4 April 2021. Finally, the convections dissipated and, thus, created the new CP over the region ($2\text{--}5^\circ\text{ N}$), which connected to north-CP. This process allows the north-CP to extend and slowly propagate southward from 05:00 to 08:00 LST on 4 April 2021 (Fig. 13b). The CP development over the north ($\text{Eq}\text{--}10^\circ\text{ N}$) is one of the mechanisms responsible for the dissipation of the north vortex and how the moisture energy transfer over the surface-level from the north across the equator to the south. It was also a reasonable factor that helped maintain the TC becomes a large Seroja TC (Fig. 14).

4 Conclusions

This work examined to investigate the physical and dynamical processes related to the tropical cyclogenesis of Seroja on 4 April 2021, which was recorded as the first Tropical Cyclone (TC) that occurred over the mainland and close to the equatorial region at the Indonesia Maritime Continent. The precondition of the tropical cyclogenesis was initiated from the local seas of eastern Indonesia (i.e., Maluku-Banda Seas). The tropical cyclogenesis could be developed by four main factors as follow:

1. The double of ITCZs may allow the convergence zone was formed over the southern part of Indonesia, despite in April the ITCZ should locate over the north equator. These double ITCZs, consistent with previous work, stated that the position of the ITCZ may be related to the TC location [5];[6]. Moreover, a previous study also demonstrated that during the double ITCZs phenomena, the deep convection and precipitation tend to be closer to the equator comparing the south and the north of ITCZs [3];[33].
2. The short-time marine heatwave (MHW) concentrated over the Maluku Sea. The warming SST has been proven in previous studies to contribute to the typhoon by changing the rainfall distribution more concentrated over the mainland than ocean regions [35].

3. The double vortices (i.e., the north-vortex and the south-vortex) with a perfect twin formation occurred over east Indonesia. Those vortices over eastern Indonesia may be attributed to the ER wave features, which correspond to the previous work [27]. In addition, during the genesis period, the maximum of meridional surface wind for the north-vortex and the south-vortex are 8 m s^{-1} and 6 m s^{-1} , respectively, which favor criteria of wind speed threshold (5 m s^{-1}) for the initial vortex to rotate the convection and amplified the cyclonic of relative vorticity [33].
4. Interaction of the eastward propagation of MJO and the westward propagation of the ER over the target domain of east Indonesia (120° S , east Nusa Tenggara) may help maintain the tropical cyclogenesis. This result consistent with previous several studies have mentioned that the wave-train was the most influencing factor for developing the TC [3];[7];[6]. In addition, over the western-north Pacific, the recently study also demonstrated that while ER wave breaking it might produce inflow to the upper-level potential vorticity and intensified the convective activity moving southwestward and, thus, triggered the tropical cyclogenesis [36].

This study suggested the interaction between the MJO and the ER help to maintain a steady blocking circulation associated with the double vortices' depiction. However, since the north-vortex starts to dissipate, it also has a role in creating the new low-level circulation over the equator and transferring the moisture energy from north to the south over the surface level under the cold pool mechanism. Thus, the mechanism provides favorable conditions to endure the tropical storm to be a Seroja tropical cyclone.

Due to the short time of extreme MHW phenomena under the global warming condition, which tend to significantly increase in terms of its intensity and frequency [31], the tropical cyclogenesis over the local seas of Indonesia is also probable expected to increase. Moreover, the circulation over the Western Pacific associated with the eastward propagation of MJO that intensified and extended during the last two decades [37] also provides the prominent circulation to maintain the tropical cyclogenesis.

If the favorable conditions needed to support the tropical cyclogenesis collocated, it is possible for the tropical cyclogenesis to reoccur in the future over the exact location in this study. It is also important to note that the WRF model with a 3 km resolution could capture the tropical cyclogenesis processes; however, the precipitation is consistently under-estimated. It was suggested that, for better predicting, the SST input [27] and the initial data from the global model needed to be regularly updated at least every six hours

Declarations

Acknowledgment

This work supports the international program of Years of the Maritime Continent (YMC) of 2017-2021. The results also support improving the forecasting product of the Satellite-based Disaster Early Warning System (SADEWA) at the Research Center for Climate and Atmosphere. The modeling simulations described in this study were completed on the High Performing Computing from the Computational

Laboratory of Atmospheric Numerical Prediction (KRESNA) at the Research Center for Climate and Atmosphere, National Research and Innovation Agency (BRIN).

Authors contribution

EY and IF are the main contributors to this manuscript who drafted the initial manuscript, revised it, improved analysis and discussions of the overall content of the manuscript, and provided simulated data and significant data findings. In addition, others contributed to the production of related figures to validate the model from satellite and reanalysis data and produced additional analysis. Finally, all the authors were involved in discussions and read and approved the final manuscript during the review process.

Conflict of interest

The authors do not have any competing interests.

Funding

The authors declare that no funds, grants, or other support were received during the preparation of this manuscript.

References

1. Tang, B. H., Fang, J., & Bentley, A. Recent advances in research on tropical cyclogenesis. *Tropical Cyclone Research and Review*, 9, 87–105, <https://doi.org/10.1016/j.tccr.2020.04.004> (2020).
2. Briegel, L. S., & Frank, W. M. Large-scale influences on tropical cyclogenesis in the Western North Pacific, *Monthly Weather Review*, 125, 1397–1413 (1997).
3. Dhavale, S., Koll, R. M., Mujumdar, M., & Singh, V. Tropical Cyclones over the Arabian Sea during the monsoon onset phase. *International Journal of Climatology*, DOI: 10.1002/joc.7403 (2021).
4. Cao, W. C. & Chen, B. The origins of monsoons, *Journal of the Atmospheric Sciences*, 58, [https://doi.org/10.1175/1520-0469\(2001\)058<3497:TOOM>2.0.CO;2](https://doi.org/10.1175/1520-0469(2001)058<3497:TOOM>2.0.CO;2) (2001).
5. Cao, X., Chen, G., & Chen, W. Tropical cyclogenesis induced by ITCZ breakdown in association with synoptic wave train over the western North Pacific. *Atmospheric Sciences Letter*, 14, 294–300, DOI: 10.1002/asl2.452 (2013).
6. Frank, W. M., & Roundy, P. E. The role of tropical waves in tropical cyclogenesis, *Monthly Weather Review*, 134, 2397–2417, <https://doi.org/10.1175/MWR3204.1> (2006).
7. Zhao, H. R., Yoshida, & Raga, G. B. Impact of the Madden–Julian Oscillation on Western North Pacific tropical cyclogenesis associated with large-scale patterns, *J. of Applied Meteorology and Climatology*, 54, 1413–1429, <https://doi.org/10.1175/JAMC-D-14-0254.1> (2015).
8. Rahul, R., Kuttippurath, J., Chakraborty, A., & Akhila, R. S. The inverse influence of MJO on the cyclogenesis in the north Indian Ocean, *Atmospheric Research*, 265, DOI:

- 10.1016/j.atmosres.2021.105880 (2021).
9. Schreck III, C.J., Molinari, J., & Mohr, K. I. Attributing Tropical Cyclogenesis to Equatorial Waves in the Western North Pacific, *J. of the Atmos. Sci.*, 68, 195-209, <https://doi.org/10.1175/2010JAS3396.1> (2011).
 10. Lekshmi, S., R., Chattopadhyay, Kaur, M., & Joseph, S. Role of initial error growth in the extended range prediction skill of Madden-Julian Oscillation (MJO), *Theoretical and Applied Climatology*, <https://doi.org/10.1007/s00704-021-03818-3> (2021).
 11. Lim, Y.-K., Nathan, P., Arnold, Molod, A. M., & Pawson, S. Seasonality in prediction skill of the Madden-Julian Oscillation and 4 associated dynamics in Version 2 of NASA's GEOS-S2S forecast 5 system, *Journal of Climate* (2021).
 12. Liang, Y., Fedorov, A. V., Zeitlin, V., & Haertel, P. The excitation of the Madden-Julian Oscillation in atmospheric adjustment to equatorial heating, *Journal of the Atmospheric Sciences*, <https://doi.org/10.1175/JAS-D-21-0092.1> (2021).
 13. Chang, C.-P., Liu, C.-H., & Kuo, H.-C. Typhoon Vamei: An equatorial tropical cyclone formation. *Geophysics Research Letters*, 30, 1–4, doi:10.1029/2002GL016365 (2003).
 14. Takahashi, H. G., Fukutomi, Y., & J. Matsumoto. The impact of long-lasting northerly surges of the East Asian Winter Monsoon on tropical cyclogenesis and its seasonal march, *Journal of the Meteorological Society of Japan*, 89A, 181–200, DOI:10.2151/jmsj.2011-A12 (2011).
 15. BNPB. Lebih dari 12.000 warga masih mengungsi akibat siklon tropis Seroja, <https://bnpb.go.id/berita/-update-lebih-dari-12-000-warga-masih-mengungsi-akibat-siklon-tropis-seroja>, last accessed: 24 October 2021 (15 April 2021).
 16. Nguyen, D.-Q., Renwick, J., & McGregor. On the presence of tropical vortices over the Southeast Asian Sea–Maritime Continent region, *Journal of Climate*, 29, 4793–4800 (2016).
 17. Bessho, K., Date, K., Hayashi, M. et al. An introduction to himawari-8/9— Japan's new-generation geostationary meteorological satellites, *Journal of the Meteorological Society of Japan*, 94, 151–183 (2016).
 18. Kubota, T., Shige, S., Hashizume, H. et al. Global precipitation map using satellite-borne microwave radiometers by the GSMaP project: production and validation, *IEEE Transactions on Geoscience and Remote Sensing*, 45, 2259–2275 (2007).
 19. Atlas, R., Hoffman, R. N., Ardizzone J. et al. A cross-calibrated, multiplatform ocean surface wind velocity product for meteorological and oceanographic applications, *BAMS*, 92, 157– 174 (2011).
 20. Ricciardulli, L., & National Center for Atmospheric Research Staff. *Climate Data Guide: CCMP: Cross-Calibrated Multi-Platform Wind Vector Analysis*, National Oceanic and Atmospheric Administration, Washington, DC, USA (2017).
 21. Hersbach, H., Bell, B., Berrisford, P., Hirahara, S., Horányi, A., Muñoz-Sabater, J. et al. The ERA5 global reanalysis, *Q.J.R. Meteorol. Soc.*, 146, 1999–2049 (2020).
 22. Hobday, A. J., Oliver, E. C. J., & Gupta, A. S. Categorizing and naming marine heatwaves, *Ocean.*, 31, 162–173, <https://doi.org/10.5670/oceanog.2018.205> (2018).

23. Skamarock, W. C., Klemp, J. B., Dudhia, J., Gill, D. O., Barker, D., Duda, M. G. et al. A description of the advanced research WRF version 3 (NCAR/TN-475+STR). University Corporation for Atmospheric Research, doi:10.5065/D68S4MVH (2008).
24. Fonseca, R. M., Zhang, T., & Yong, K.-T. Improved simulation of precipitation in the tropics using a modified BMJ scheme in the WRF model. *Geosciences Model Development*, 8, 2915–2928 (2015).
25. Yulihastin, E., Fathrio, I., Trismidianto, Nauval, F., Saufina, E., Harjupa, W., Satiadi, D., & Nuryanto, D. E. Convective cold pool associated with offshore propagation of convection system over the east coast of Southern Sumatra, Indonesia. *Advances in Meteorology*, 2021, 1–13, doi:10.1155/2021/2047609 (2021a).
26. Yulihastin, E., Nuryanto, D. E., Trismidianto, Muharsyah, R. Improvement of heavy rainfall simulated with SST adjustment associated with Mesoscale Convective Complexes related to severe flash flood in Luwu, Sulawesi, Indonesia. *Atmos.*, 12, 1445, <https://doi.org/10.3390/atmos12111445>, (2021b).
27. Lubis, S. W., & Respati, M. R. Impacts of convectively coupled equatorial waves on rainfall extremes in Java, Indonesia, *International Journal of Climatology*, 1–23, DOI: 10.1002/joc.6967 (2020).
28. Rui, H., & Wang, B. Development characteristics and dynamic structure of tropical intraseasonal convection anomalies, 47, 357–379 (1990).
29. Liang, M., Chan, J. C. L., J. Xu et al. Numerical prediction of tropical cyclogenesis part I: Evaluation of model performance, *Quarterly Journal of the Royal Meteorology Society*, <https://doi.org/10.1002/qj.3987> (2021).
30. Frölicher, T. L., Fischer, E. M., & Gruber, N. Marine heatwaves under global warming, *Nature*, 560, 360–364 (2018).
31. Hague, B. S. Seasonal climate summary for Australia and the southern hemisphere (summer 2018–19): extreme heat and flooding prominent, *Journal of Southern Hemisphere Earth Systems Science*, 71, 147–158, <https://doi.org/10.1071/ES20009> (2021).
32. Kilroy, G., Smith, R. K., & Montgomery, M. T. A unified view of tropical cyclogenesis and intensification, *Quarterly Journal of the Royal Meteorology Society*, 143, 450–462, DOI:10.1002/qj.2934 (2017).
33. Chen, B., Lin, X., & Bacmeister, J. T. Frequency distribution of daily ITCZ patterns over the Western–Central Pacific, 21, 4207–4222, DOI: 10.1175/2008JCLI1973.1 (2008).
34. Haffke, C., Magnusdottir, G., Henke, D., Smyth, P. & Peings, Y. Daily states of the March–April east Pacific ITCZ in three decades of high-resolution satellite data, *Journal of Climate*, 29, 2981–2995 (2016).
35. Iizuka, S., Kawamura, R., Nakamura, H., & Miyama, T. Influence of warm SST in the Oyashio region on rainfall distribution of Typhoon Hagibis, *SOLA*, 17A, 21 – 28, <https://doi.org/10.2151/sola.17A-004> (2019).
36. Takemura, K., & Mukaugawa, H. Tropical cyclogenesis triggered by Rossby wave breaking over the Western North Pacific, *SOLA*, 17, 164–169 (2021).

37. Yu, H., Fu, Z., and Franzke, C. L. E. A Secular Shift of the Madden-Julian Oscillation and Its Relation to Western Pacific Ocean, *Geophysics Research Letters*, 48, e2021GL095400. <https://doi.org/10.1029/2021GL095400> (2021).

Figures

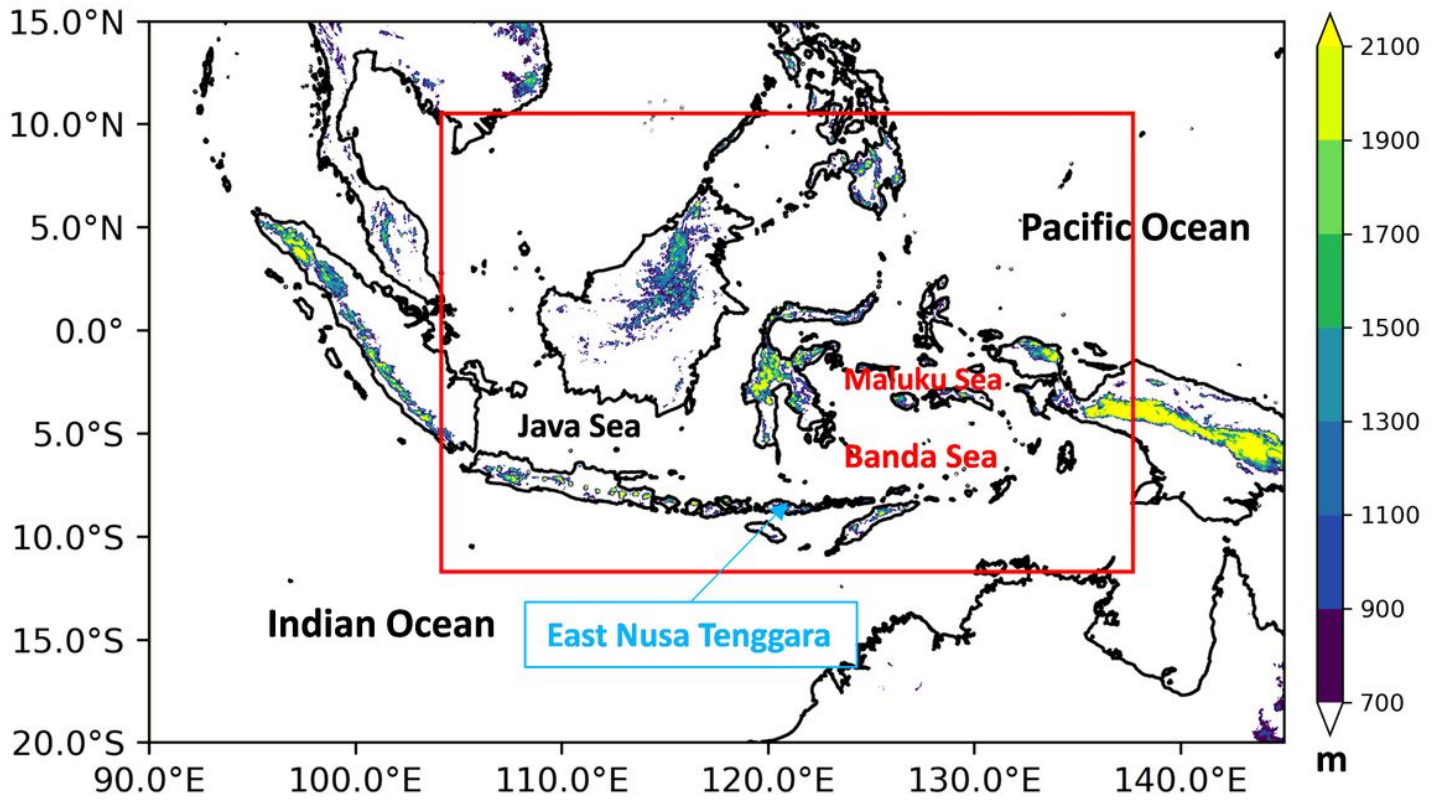


Figure 1

Configuration of model domain (red box) for simulating tropical cyclogenesis over the eastern Maritime Continent with horizontal resolutions of 3 km.

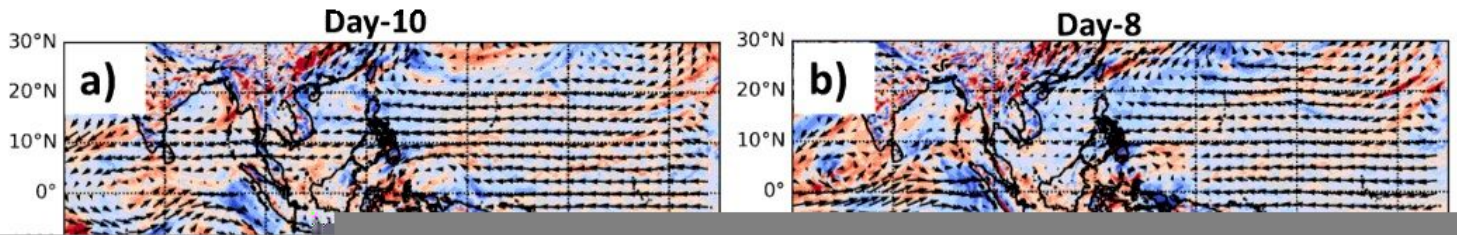


Figure 2

Time evolution of wind vector overlaid with wind divergence (shaded) at 850 mb with positive (negative) values indicated divergence (convergence) over the Maritime Continent derived from ERA5 reanalysis data for: (a-f) day-10 to day-0 with day-0 denoted as 4 April 2021 which associated with the catastrophic disaster event over Flores, eastern Nusa Tenggara, Indonesia.

Figure 3

As Figure 2, but for domain area refer to Figure 1 (red box).

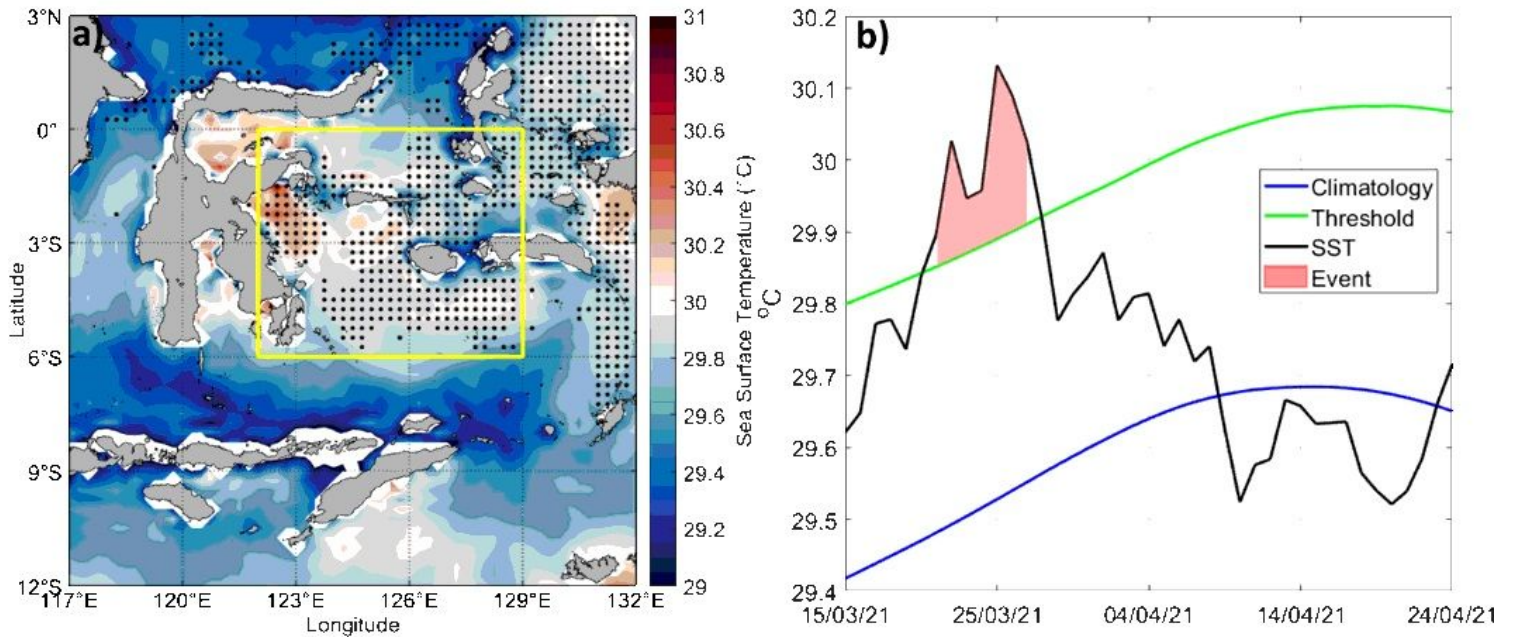


Figure 4

(a) A map showing distribution of sea surface temperature (SST) average from 23 March–4 April 2021. Black dot indicated marine heatwave event based on SST > threshold. Yellow box represents area used in the Figure 4b. (b) Time series of SST data for: climatology of daily SST during April (blue line), moving threshold of marine heatwave following Konopka et al. (2016) (green line), daily SST (black line), SST > threshold indicated as marine heatwave event (pink shaded).

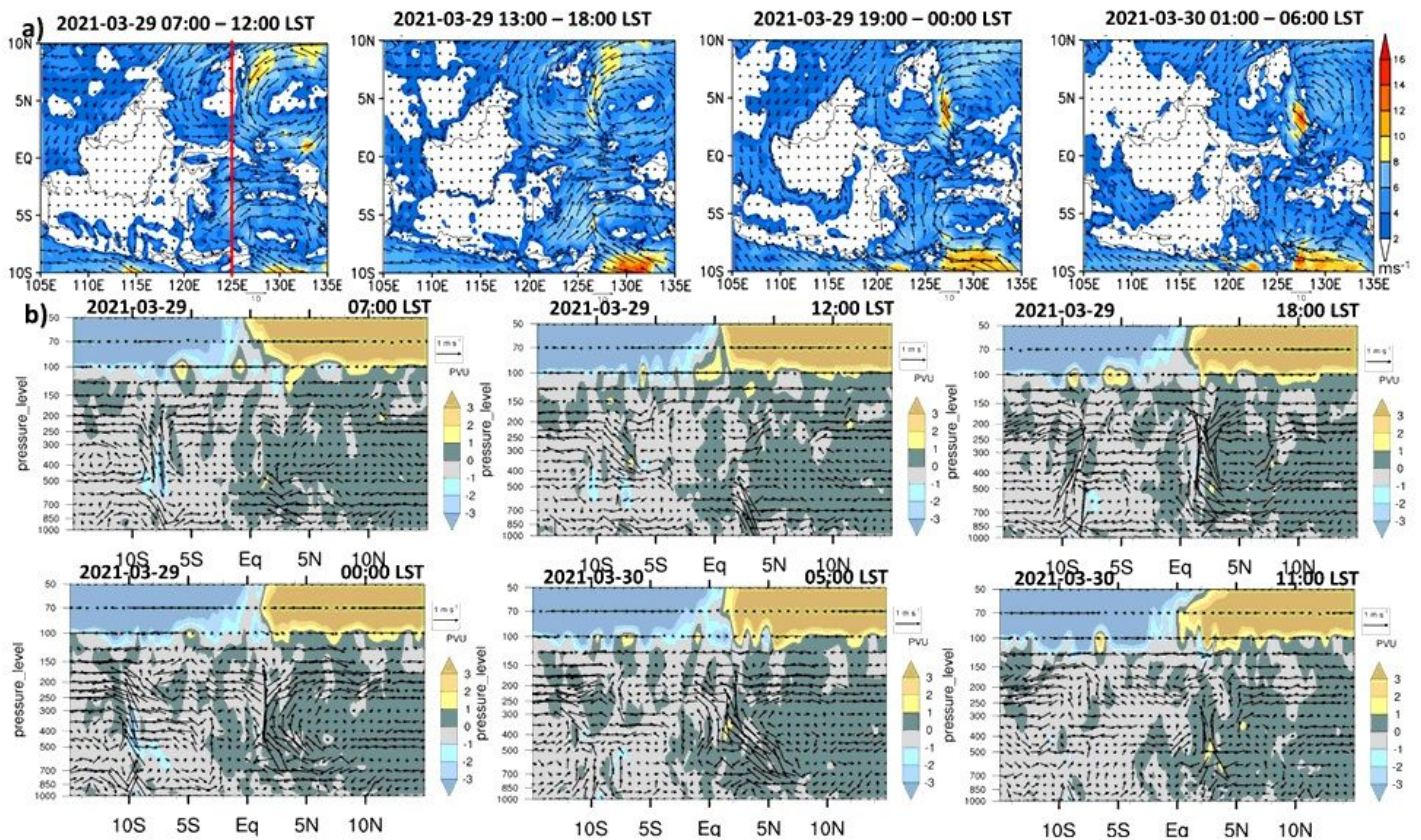


Figure 5

(a) Time evolution of a spatial map of 6-hourly average wind surface data from CCMP on 29–30 March 2021. (b) Vertical-latitude cross section of potential vorticity (shaded) and meridional wind (vector) from ERA5 data along longitude of 125°E refer to red vertical line in Figure 5 (a).

Figure 6

(a) A Hovmöller diagram of Time-Latitude cross section averaged over $120^{\circ}\text{--}130^{\circ}\text{E}$ during 15 March–30 April 2021 for a low-level divergence at 925 mb, (b) as (a), but for potential vorticity, (c) as (a), but for A Time-Longitude cross section averaged over $15^{\circ}\text{S--}15^{\circ}\text{N}$ for OLR anomalies based on monthly average data of March–April 2021, (d) as (c), but for total column water vapor anomalies. The dashed black-boxes represent the meeting location between MJO and ER waves.

Figure 7

(a) Time evolution of a spatial map of 6-hourly vector and magnitude of surface wind (at 10 m) derived from CCMP data (left-side) and WRF (right-side) from 3 April 2021 on 19:00 LST to 4 April 2021 on 18:00

LST derived from (a) GSMAp satellite, (b) WRF model.

Figure 8

Vertical-longitude cross section of wind (vector; zonal component multiplied by a factor of 0.01), equivalent potential temperature (contour), and cloud mixing ratio (shaded) along the thick black horizontal line from point A to point B in Figure 10(b) with time evolution for: (a) 4 April 2021 from 01:00 – 08:00 LST. The X-axis is longitude representing the distance of A-B transect. For clarity, the equivalent potential temperatures (θ_e) are differenced as contour lines with red for $\theta_e \geq 350$ K, blue for $350 > \theta_e \geq 345$ K, and purple for $345 > \theta_e \geq 340$ K. The simulated data derived from the WRF model.

Figure 9

As Figure 7, but for meridional wind vector and potential vorticity (shaded). The vector wind is meridional component multiplied by a factor of 0.01 derived from ERA5 data.